Supplementary Information

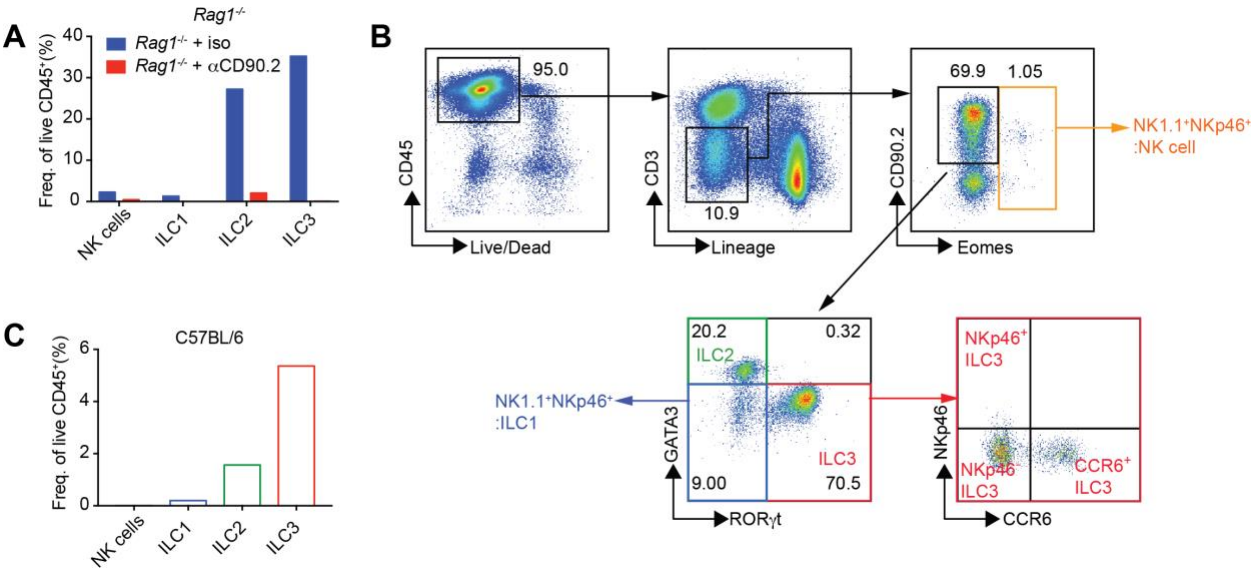

Figure S1, related to Figure 1. Frequencies of small intestinal ILC subsets from αCD90.2 treated mice and gating strategy for intestinal ILC subsets. (A) Frequencies of small intestinal ILC subsets from αCD90.2 treated and control mice. Gating was performed, as described below. (B) Gating strategy for intestinal ILC subsets. SI-LPL were stained and analyzed by flow cytometry. Gating was performed on lymphocytes and doublets were excluded. Gating was performed on live $CD45^+$ cells and Lin^+ $CD3^+$ cells were excluded. Lineage markers were CD19, B220, CD11c, CD11b, Gr1. Lin^-CD3^- cells were then analyzed for intestinal ILC subsets based on previous criteria (Gronke et al., 2017). Gating strategy for NK cells ($CD45^+Lin^-CD3^-Eomes^+NK1.1^+NKp46^+$), for ILC1 ($CD45^+Lin^-CD3^-Eomes^-CD90.2^+GATA3^-ROR\gamma t^-NK1.1^+NKp46^+$), for ILC2 ($CD45^+Lin^-CD3^-Eomes^-CD90.2^+GATA3^+ROR\gamma t^-$), for ILC3 ($CD45^+Lin^-CD3^-Eomes^-CD90.2^+GATA3^-ROR\gamma t^+$), for NKp46$^+$ILC3 ($CD45^+Lin^-CD3^-Eomes^-CD90.2^+GATA3^-ROR\gamma t^+CCR6^-NKp46^+$), for NKp46$^-$ILC3 ($CD45^+Lin^-CD3^-Eomes^-CD90.2^+GATA3^-ROR\gamma t^+CCR6^-NKp46^-$), and for CCR6$^+$ILC3 ($CD45^+Lin^-CD3^-Eomes^-CD90.2^+GATA3^-ROR\gamma t^+CCR6^+NKp46^-$). (C) Frequencies of small intestinal ILC subsets from C57BL/6.

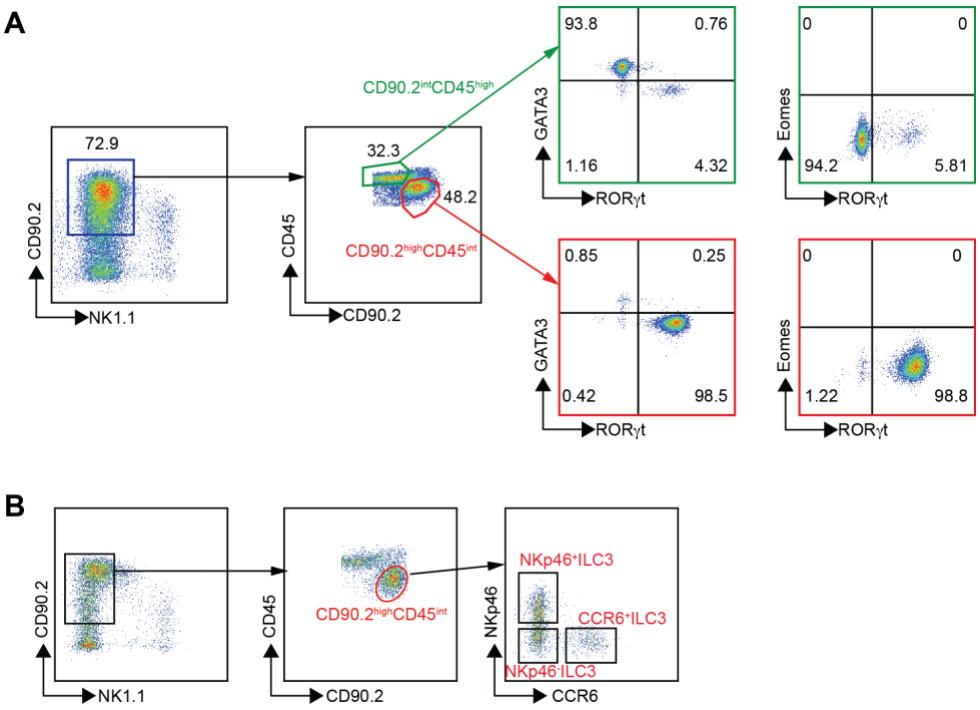

Figure S2, related to Figure 2. Gating strategy for isolation of intestinal ILC3 subsets. (A) The population of Lin$^-$CD90^{high}CD45^{int} cells was predominantly RORγt$^+$ILC3. Data show initial flow cytometry plot gated on live CD45$^+$Lin$^-$CD3$^-$CD90.2$^+$NK1.1$^-$cells (blue square) in *Rag1*$^{-/-}$ mice. (B) Gating strategy for isolation of intestinal ILC3 subsets from *Rag1*$^{-/-}$ mice. Gating was performed on live CD45$^+$Lin$^-$CD3$^-$CD90.2$^+$NK1.1$^-$cells. Next, CD90^{high}CD45^{int} cells were selected, and then divided these further based on NKp46 and CCR6 expression. Gating strategy for NKp46$^-$ILC3 (CD45$^+$Lin$^-$CD3$^-$NK1.1$^-$CD90.2^{high}CD45^{int}CCR6$^-$NKp46$^-$), NKp46$^+$ILC3 (CD45$^+$Lin$^-$CD3$^-$NK1.1$^-$CD90.2^{high}CD45^{int}CCR6$^-$NKp46$^+$), and CCR6$^+$ILC3 (CD45$^+$Lin$^-$CD3$^-$NK1.1$^-$CD90.2^{high}CD45^{int}CCR6$^+$NKp46$^-$).

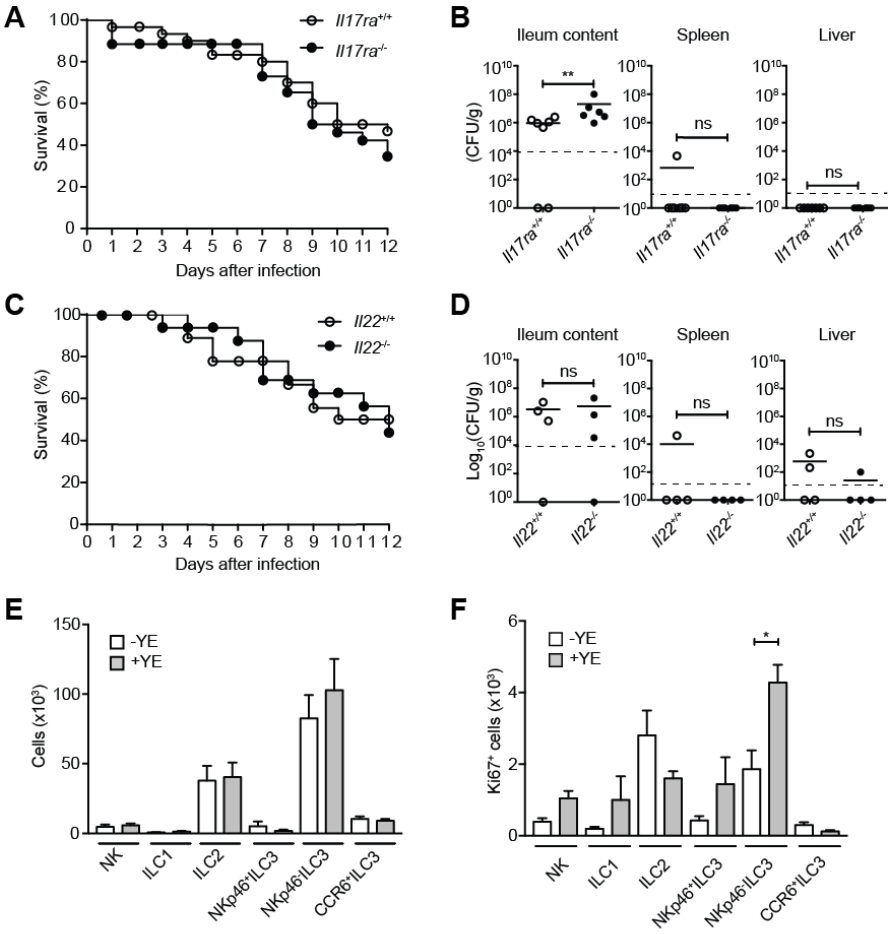

Figure S3, related to Figure 3. IL-17 and IL-22 are not required for survival from YE infection. (A-D) Groups of mice were infected orally with 1.5 x 10^8 YE CFU/mouse. (A,C) Survival curves. (B,D) Bacterial burdens at day 7 p.i. (A, n = a total of 26~30 mice per group; B, n = 6~7 per group; C, n=16~18 per group; D, n=4 per group). Bars show the mean, symbols represent individual mice. Dotted horizontal line represents the limit of detection. (E-F) C57BL/6 mice were infected orally with 1.5 x 10^8 YE CFU/mouse (n=5 per group). (E) Numbers of each ILC subset from the SI-LPL at day 3 p.i. (F) Numbers of $Ki67^+$ cells from each ILC subset at day 3 p.i. Statistical analysis was performed using Log-rank test (A,C) or Mann-Whitney test (B,D,E,F). Statistical significance is indicated by *, $p < 0.05$; ns, not significant. Data in E and F show mean±SEM. Data represent pooled results from at least two experiments (A,C) or representative results of at least two independent experiments with four mice in each experimental group (B,D,E,F).

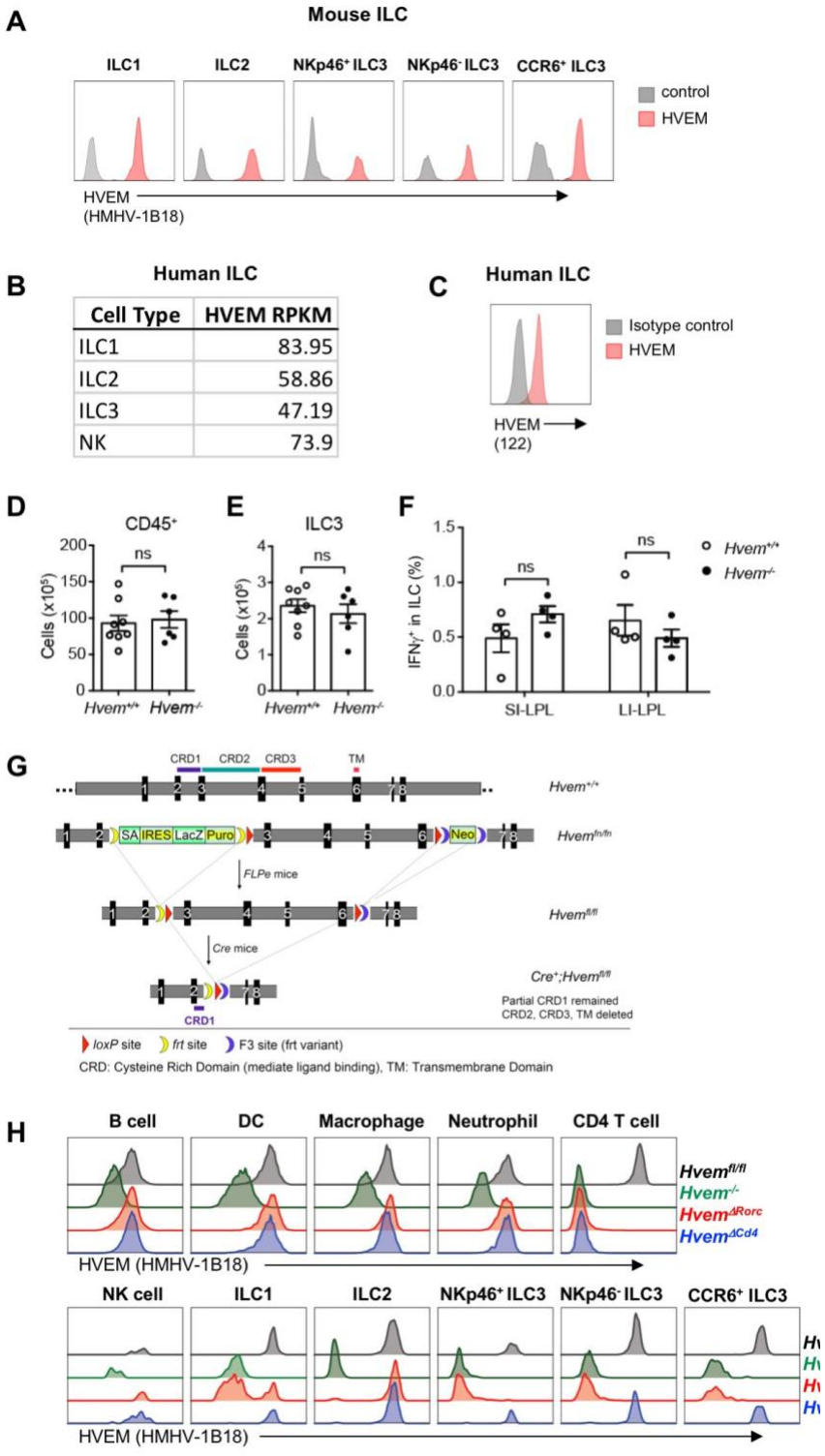

Figure S4, related to Figure 5. All subsets of ILC express HVEM. (A) HVEM expression on mouse intestinal ILC subsets. Pink shading shows the level of HVEM expression on each subset of ILC. Gray shading is the negative control (*Hvem*$^{-/-}$ mice).

(B) mRNA expression of *Hvem* by each ILC population from human tonsils. Single cell RNA-Seq was performed on human ILC1, ILC2, ILC3 and NK cells by Björkland et al. (Bjorklund et al., 2016). Gene expression was determined in the form of reads per kilobase per million mapped reads (RPKM). Average levels of *Hvem* were determined by including all 648 sequenced cells (GSE70580; 127 ILC1, 139 ILC3, 308 ILC3 and 74 NK cells). Of note, previous reports state that a minimum RPKM threshold of 10 (or less) adequately eliminates noise associated with sequencing (Glaus et al., 2012; Ramskold et al., 2009), suggesting that HVEM is actively being expressed by all 4 human ILC subsets. (C) HVEM expression on human ILC (live $CD45^+Lin^-CD94^-CD127^+$) from PBMC. Flow cytometry based gating strategy from the reference (Simoni et al., 2017). Lineage markers were CD3, CD19, CD4, CD8, CD16, CD34. Pink shading shows the level of HVEM expression on human ILC. Gray shading is the isotype control. (D-E) Absolute numbers of total lymphocytes (D) and ILC3 ($CD45^+Lin^-CD3^-CD90.2^+ROR\gamma t^+$) (E) from ileal LPL of $Hvem^{+/+}$ and $Hvem^{-/-}$ mice. Data represents pooled results from at two experiments. (F) Frequencies of IFNγ-expressing ILC from ileal LPL isolated from $Hvem^{+/+}$ and $Hvem^{-/-}$ mice. Representative results of at least two independent experiments with at least four mice in each experimental group. (G-H) *Hvem* gene targeting to generate *Hvem* conditional KO mice. (G) Mouse *Hvem* genomic locus is shown (uppermost). Germline transmitted mice ($Hvem^{flox\text{-}neo/flox\text{-}neo}$ = $Hvem^{fn/fn}$, knockout first) were crossed with *FLPe* mice to delete the Neo^r cassette to generate $Hvem^{fl/fl}$ mice. $Hvem^{fl/fl}$ mice were bred to Cre-expressing mice to generate conditional knockout mice. (H) Expression of HVEM on SI-LP from WT ($Hvem^{fl/fl}$), $Hvem^{-/-}$ ($Hvem^{fn/fn}$), $Hvem^{\Delta Rorc}$ (*Rorc-Cre* × $Hvem^{fl/fl}$) and $Hvem^{\Delta Cd4}$ (*Cd4-Cre* × $Hvem^{fl/fl}$ *mice)*. Analysis of HVEM expression in B cells ($CD45^+B220^+CD19^+$), DC ($CD11b^+CD11c^{hi}$), macrophages ($CD11b^+F4/80^+$), neutrophils ($CD11b^+Gr1^{hi}$), CD4 T cells ($CD45^+Lin^-CD3^+CD4^+$), NK cells, ILC1, ILC2, $NKp46^+$ILC3, for $NKp46^-$ILC3 and $CCR6^+$ILC3. Results are representative of at least two independent experiments. Statistical analysis was performed using Mann-Whitney test (D-F). Statistical significance is indicated by ns, not significant.

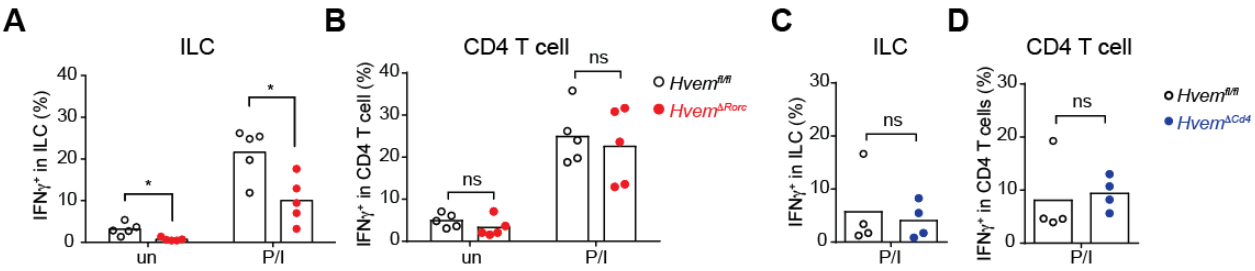

Figure S5, related to Figure 6. HVEM deficient ILC are impaired for protective cytokine production. (A-D) Frequencies of IFNγ-expressing ILC and CD4 T cells from ileal LPL isolated from *Hvem*$^{\Delta Rorc}$ (A,B) and *Hvem*$^{\Delta Cd4}$ (C,D) mice at day 7 p.i. (A-B, 1.2 x 10^8 YE CFU/mouse; C-D, 2 x 10^8 YE CFU/mouse). Cells were either unstimulated (un) or P/I and BFA was added in the last 2h of incubation before analysis for intracellular cytokines. Statistical analysis was performed using Mann-Whitney test. Statistical significance is indicated by *, $p < 0.05$; ns, not significant. Bars show the mean, symbols represent individual mice. Data represents pooled results from at two experiments (A,B) or representative results of at least two independent experiments with at least four mice in each experimental group (C,D).

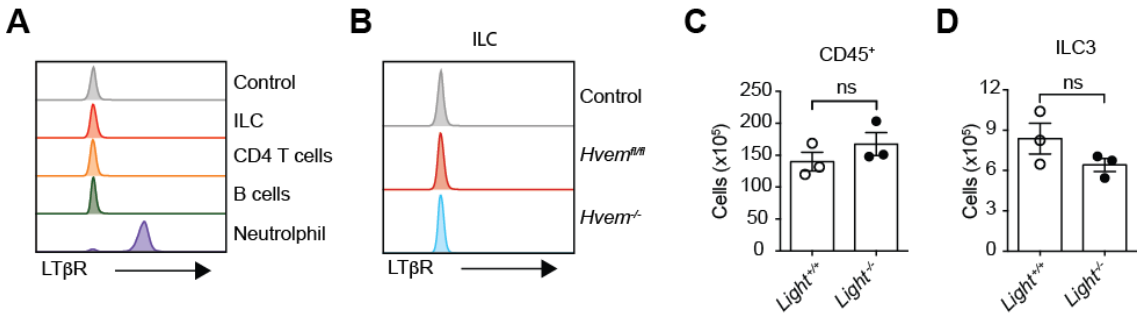

Figure S6, related to Figure 7. Expression of the LTβR on ILC and the number of SI-ILC3 from *Light*$^{-/-}$ mice. (A) Expression of the LTβR by mAb staining of ILC, CD4 T cells, B cells and neutrophils with negative controls (gray shading) provided by cells from *Ltbr*$^{-/-}$ mice. (B) Comparison of the level of LTβR expression on intestinal ILC from *Hvem*$^{-/-}$ mice and control mice. (C-D) Absolute numbers of total lymphocytes (C) and ILC3 ($CD45^+Lin^-CD3^-CD90.2^+ROR\gamma t^+$) (D) from SI-LP of co-housed *Light*$^{-/-}$ and *Light*$^{+/+}$ mice (n=3 per group). Bar graphs show mean±SEM. Statistical significance is indicated by ns, not significant. Statistical analysis was performed using Mann-Whitney test.

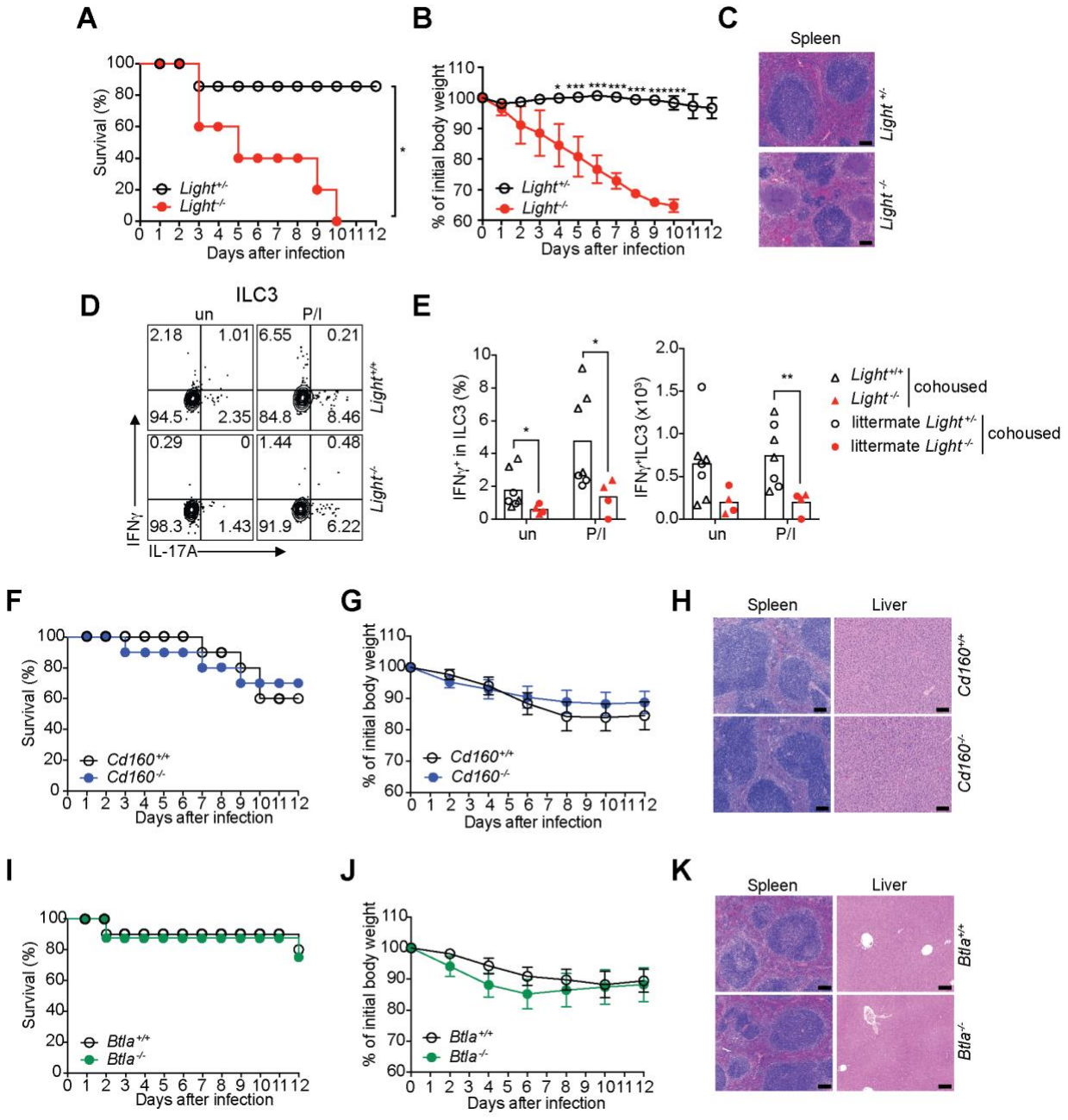

Figure S7, related to Figure 7. BTLA and CD160 are not required for host defense against YE. (A-E) Co-housed littermate or co-housed *Light*$^{-/-}$ mice and control mice were infected orally with YE. (A) Survival curves. (B) Changes in body weight. (A-B,1.6 x 10^8 YE CFU/mouse; n=5-7 per group; co-housed littermates). (C) Representative H&E-stained splenic tissue sections from the indicated mice at day 3 p.i. (1.2x10^8 YE CFU/mouse; n=3 per group; co-housed littermates). Scale bars, 100μm. (D-E) Representative plots of IFNγ and IL-17A expression by ILC3 (CD45$^+$Lin$^-$CD3$^-$Eomes$^-$

CD90.2^{+}GATA3^{-}RORγt^{+}). (D) and frequencies and absolute numbers of IFNγ^{+} expressing ILC3 (E) from SI-LP isolated from co-housed (triangles) or co-housed littermates (circles) control and *Light*$^{-/-}$ mice at day 3 p.i. Cells were either unstimulated (un) or stimulated for 4h with P/I and BFA was added in the last 2h of incubation before analysis for transcription factors and cytokines (1.2~1.6x10^{8} YE CFU/mouse; n=4-7 per group; co-housed or co-housed littermates). Bars show the mean and symbols represent individual mice. (F-K) Groups of mice were infected orally with 1.0 x 10^{8} YE CFU (E-G, n=8-10 per group, co-housed littermates; H-J, n=10 per group, co-housed). (F,I) Survival curves. (G,J) Changes in body weight. (H,K) Representative H&E-stained tissue sections from the indicated mice at day 7 p.i. Scale bars, 100μm. Statistical significance is indicated by *, $p < 0.05$; **, $p < 0.01$; ***, $p < 0.001$. Statistical analysis was performed using Log-rank test (A,F,I) and 2 way ANOVA with Bonferroni's multiple hypothesis correction (B,G,J), or Mann-Whitney test (E). Data shown are mean±SEM (B,G,J). Data represent pooled results from two experiments (A-B,E) or representative results of at least two independent experiments in each experimental group (F-K).